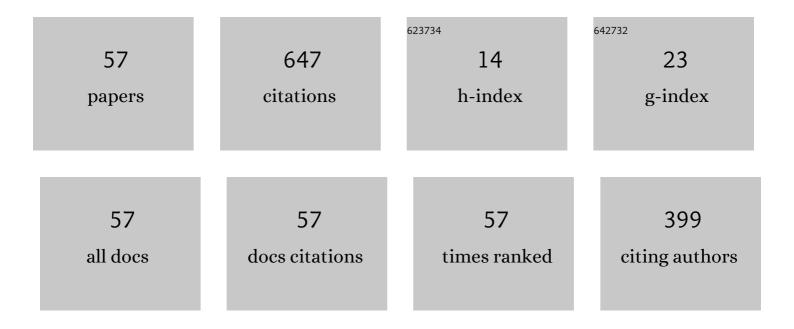
## Keiji Tsukada

List of Publications by Year in descending order

Source: https://exaly.com/author-pdf/1615782/publications.pdf Version: 2024-02-01



Κειιι Τοιικληλ

#	Article	IF	CITATIONS
1	Small Eddy Current Testing Sensor Probe Using a Tunneling Magnetoresistance Sensor to Detect Cracks in Steel Structures. IEEE Transactions on Magnetics, 2018, 54, 1-5.	2.1	50
2	Detection of Inner Cracks in Thick Steel Plates Using Unsaturated AC Magnetic Flux Leakage Testing With a Magnetic Resistance Gradiometer. IEEE Transactions on Magnetics, 2017, 53, 1-5.	2.1	46
3	Detection of Inner Corrosion of Steel Construction Using Magnetic Resistance Sensor and Magnetic Spectroscopy Analysis. IEEE Transactions on Magnetics, 2016, 52, 1-4.	2.1	45
4	A magnetic flux leakage method using a magnetoresistive sensor for nondestructive evaluation of spot welds. NDT and E International, 2011, 44, 101-105.	3.7	44
5	Detection of back-side pit on a ferrous plate by magnetic flux leakage method with analyzing magnetic field vector. NDT and E International, 2010, 43, 323-328.	3.7	34
6	Fourier-transformed eddy current technique to visualize cross-sections of conductive materials. NDT and E International, 2007, 40, 363-367.	3.7	29
7	Magnetic property mapping system for analyzing three-dimensional magnetic components. Review of Scientific Instruments, 2006, 77, 063703.	1.3	26
8	Highly Sensitive Third-Harmonic Detection Method of Magnetic Nanoparticles Using an AC Susceptibility Measurement System for Liquid-Phase Assay. IEEE Transactions on Applied Superconductivity, 2016, 26, 1-4.	1.7	25
9	Magnetic Measurement of Moisture Content of Grain. IEEE Transactions on Magnetics, 2007, 43, 2683-2685.	2.1	21
10	Highly Sensitive Measurement of Moisture Content Using HTS-SQUID. IEEE Transactions on Applied Superconductivity, 2009, 19, 878-881.	1.7	20
11	Difference in the detection limits of flaws in the depths of multi-layered and continuous aluminum plates using low-frequency eddy current testing. NDT and E International, 2008, 41, 108-111.	3.7	19
12	Magnetic thickness gauge using a Fourier transformed eddy current technique. NDT and E International, 2009, 42, 606-609.	3.7	17
13	Effect of diamagnetic contribution of water on harmonics distribution in a dilute solution of iron oxide nanoparticles measured using high-Tc SQUID magnetometer. Journal of Magnetism and Magnetic Materials, 2015, 394, 260-265.	2.3	16
14	Imaging of Defect Signal of Reinforcing Steel Bar at High Lift-Off Using a Magnetic Sensor Array by Unsaturated AC Magnetic Flux Leakage Testing. IEEE Transactions on Magnetics, 2021, 57, 1-4.	2.1	14
15	Detection of the weak magnetic properties change of stainless-steel welding parts by low frequency magnetic imaging. Journal of Applied Physics, 2008, 103, .	2.5	13
16	Eddy Current Testing System Using HTS-SQUID With External Pickup Coil Made of HTS Wire. IEEE Transactions on Applied Superconductivity, 2017, 27, 1-5.	1.7	13
17	Development of Eddy Current Testing System Using HTS-SQUID on a Hand Cart for Detection of Fatigue Cracks of Steel Plate Used in Expressways. IEEE Transactions on Applied Superconductivity, 2018, 28, 1-5.	1.7	13
18	Using Magnetic Field Gradients to Shorten the Antigen-Antibody Reaction Time for a Magnetic Immunoassay. IEEE Transactions on Magnetics, 2019, 55, 1-5.	2.1	13

Keiji Tsukada

#	Article	IF	CITATIONS
19	Optimization of an AC/DC High- <inline-formula> <tex-math notation="TeX">\$T_{m c}\$</tex-math></inline-formula> SQUID Magnetometer Detection Unit for Evaluation of Magnetic Nanoparticles in Solution. IEEE Transactions on Applied Superconductivity, 2015, 25, 1-4.	1.7	12
20	Imaging of Chemical Reactions Using a Terahertz Chemical Microscope. Photonics, 2019, 6, 10.	2.0	12
21	Integrated Magnetic Sensor Probe and Excitation Wire for Nondestructive Detection of Submillimeter Defects. IEEE Magnetics Letters, 2019, 10, 1-5.	1.1	11
22	Electric Potential Distribution on Lithium Ion Battery Cathodes Measured Using Terahertz Chemical Microscopy. Journal of Infrared, Millimeter, and Terahertz Waves, 2020, 41, 430-437.	2.2	11
23	A Proton Pumping Gate Field-Effect Transistor for a Hydrogen Gas Sensor. IEEE Sensors Journal, 2007, 7, 1268-1269.	4.7	9
24	Non-Contact Thickness Gauge for Conductive Materials Using HTS SQUID System. IEEE Transactions on Applied Superconductivity, 2009, 19, 801-803.	1.7	9
25	Hybrid Type HTS-SQUID Magnetometer With Vibrating and Rotating Sample. IEEE Transactions on Applied Superconductivity, 2016, 26, 1-5.	1.7	8
26	Absolute-magnetic-field measurement using nanogranular in-gap magnetic sensor with second-harmonic and liquid-nitrogen-temperature operation. AIP Advances, 2017, 7, 056670.	1.3	8
27	Extraction Method of Crack Signal for Inspection of Complicated Steel Structures Using A Dual-Channel Magnetic Sensor. Sensors, 2019, 19, 3001.	3.8	8
28	Investigation and repair plan for abraded steel bridge piers: case study from Japan. Proceedings of the Institution of Civil Engineers: Forensic Engineering, 2019, 172, 11-18.	0.5	8
29	Low-frequency magnetic field detection for metal sensing. International Journal of Applied Electromagnetics and Mechanics, 2007, 25, 447-451.	0.6	7
30	An MFL Probe using Shiftable Magnetization Angle for Front and Back Side Crack Evaluation. , 2019, , .		7
31	Influence of Viscosity on Dynamic Magnetization of Thermally Blocked Iron Oxide Nanoparticles Characterized by a Sensitive AC Magnetometer. Journal of Superconductivity and Novel Magnetism, 2019, 32, 2765-2772.	1.8	6
32	Development of a Highly Sensitive Magnetic Field Detector With a Wide Frequency Range for Nondestructive Testing Using an HTS Coil With Magnetic Sensors. IEEE Transactions on Applied Superconductivity, 2019, 29, 1-5.	1.7	6
33	Hybrid Magnetic Sensor Combined With a Tunnel Magnetoresistive Sensor and High-Temperature Superconducting Magnetic-Field-Focusing Plates. IEEE Transactions on Applied Superconductivity, 2019, 29, 1-5.	1.7	6
34	A Low-Frequency Eddy Current Probe Based on Miniature Fluxgate Array for Defect Evaluation in Steel Components. IEEE Transactions on Magnetics, 2022, 58, 1-5.	2.1	6
35	Extraction of Flux Leakage and Eddy Current Signals Induced by Submillimeter Backside Slits on Carbon Steel Plate Using a Low-Field AMR Differential Magnetic Probe. IEEE Access, 2021, 9, 146755-146770.	4.2	6
36	Evaluation of the Magnetization Properties of Magnetic Nanoparticles in Serum Using HTS-SQUID. IEEE Transactions on Applied Superconductivity, 2018, 28, 1-5.	1.7	5

Keiji Tsukada

#	Article	IF	CITATIONS
37	Anisotropy magnetoresistance differential probe for characterization of sub-millimeter surface defects on galvanized steel plate. Measurement and Control, 2021, 54, 1273-1285.	1.8	5
38	Magnetic image detection of the stainless-steel welding part inside a multi-layered tube structure. NDT and E International, 2009, 42, 308-315.	3.7	4
39	Application of a HTS Coil With a Magnetic Sensor to Nondestructive Testing Using a Low-Frequency Magnetic Field. IEEE Transactions on Applied Superconductivity, 2017, 27, 1-4.	1.7	4
40	Magnetic Detection of Steel Corrosion at a Buried Position Near the Ground Level Using a Magnetic Resistance Sensor. IEEE Transactions on Magnetics, 2018, 54, 1-4.	2.1	4
41	Crack Detection for Welded Joint With Surface Coating Using Unsaturated AC Magnetic Flux Leakage. IEEE Transactions on Magnetics, 2022, 58, 1-5.	2.1	4
42	Magnetic characterization change by solvents of magnetic nanoparticles in liquid-phase magnetic immunoassay. AIP Advances, 2019, 9, .	1.3	3
43	Properties of single- and multi-core magnetic nanoparticles assessed by magnetic susceptibility measurements. Journal of Magnetism and Magnetic Materials, 2021, 528, 167812.	2.3	3
44	Development of impedance measurement of lithium ion batteries electrode using terahertz chemical microscope. Electrical Engineering in Japan (English Translation of Denki Gakkai Ronbunshi), 2021, 214, e23355.	0.4	3
45	Magnetic thickness measurement for various iron steels using magnetic sensor and effect of electromagnetic characteristics. AIP Advances, 2022, 12, .	1.3	3
46	Magnetic characteristics measurements of ethanol–water mixtures using a hybrid-type high-temperature superconducting quantum-interference device magnetometer. AIP Advances, 2017, 7, 056707.	1.3	2
47	Development of Three-Channel HTS-SQUID Inspection System for Orthotropic Steel Decks of Expressway Bridges. IEEE Transactions on Applied Superconductivity, 2019, 29, 1-5.	1.7	2
48	Laser monitoring of dynamic behavior of magnetic nanoparticles in magnetic field gradient. AIP Advances, 2020, 10, .	1.3	2
49	Development of Impedance Measurement of Lithium Ion Batteries Electrode using Terahertz Chemical Microscope. IEEJ Transactions on Sensors and Micromachines, 2021, 141, 273-278.	0.1	2
50	Sensitivity Improvement of Sample Rotation Measurement Method in HTS-SQUID Magnetometer for Diamagnetic Materials. IEEE Transactions on Applied Superconductivity, 2018, 28, 1-4.	1.7	1
51	Evaluation of Bio-materials Using a Laser-excited Terahertz Wave. Nippon Laser Igakkaishi, 2019, 39, 341-346.	0.0	1
52	A benchtop induction-based AC magnetometer for a fast characterization of magnetic nanoparticles. Engineering Research Express, 2022, 4, 025047.	1.6	1
53	Laser-terahertz emission from the chemical sensing plate. , 2007, , .		0
54	Hydrogen-Gas Detection System and its Functions to Make Each Sensor Wireless. IEEJ Transactions on Electrical and Electronic Engineering, 2008, 3, 229-235.	1.4	0

#	Article	IF	CITATIONS
55	Evaluation of Li-ion battery using a Terahertz Chemical Microscope. , 2018, , .		Ο
56	A sensitive magnetometer utilizing high-Tc SQUID for magnetic property characterization. Microsystem Technologies, 2021, 27, 3413-3420.	2.0	0
57	Reduction of Wind Disturbance by Optimizing the Drive Current of Pt Ultra-thin Film Hydrogen Sensor. IEEJ Transactions on Sensors and Micromachines, 2020, 140, 92-96.	0.1	Ο